Journal of Geomine (2023), 1(2), 56-67
DOI: 10.22077/jgm.2023.6431.1007

Minerals chemistry and petrogenesis of metamorphic rocks of Anjul area, southwest of Qayen

Gholamreza Fotoohi Rad[1], Mohammad Hossein Yousefzadeh[2], Hossein Najafi Shahali Bagloo[3]

Recived: 2023 May. 30, Revised: 2023 Aug. 04, Online Published: 2023 Aug. 11

ABSTRACT

The study area is a part of the Sistan suture zone of eastern Iran that is located in the southwest of Qayen city with a northwest-southeast extension. The studied rocks were affected by the regional metamorphism with low to high metamorphism intensity variables. This metamorphism has produced greenschist, amphibolite, and granulite facies rocks. Mineral chemistries indicate that amphiboles of the studied metamorphic rocks were magnesiohornblende and are categorized as metamorphic amphiboles. Pyroxenes are of Augite type, plagioclases are at the level of andesine to labradorite, and biotites are of types that are rich in iron. Definite chemical zoning of garnets in studied metamorphic rocks of the area is the indicator of their formation and development during increasing pressure and temperature that is evidence of Subduction and the rise of a part of the metamorphic rocks during thrust faulting in a direction opposite to that of Subduction in the study area.

KEYWORDS

Petrology, Anjul, Lut Block, Sistan suture zone

I. INTRODUCTION AND THE GEOLOGICAL STUDY

The study area is located in the north of South Khorasan Province in the east of Iran and the northwest margin of Sistan suture zone and northeast of Lut block (Tirrul et al. 1983; Sadat, 1978) (Fig. 1).

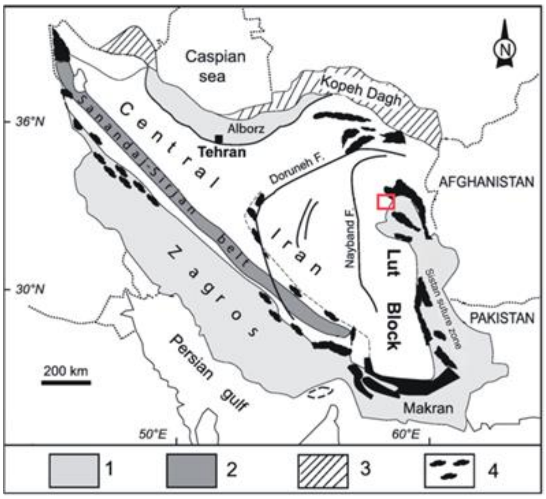

Fig. 1. The location of the study area(square) in the classification of structural zones in Iran 1. Zagros, 2. Sanandaj – Sirjan Belt, 3. Kopet dagh, 4. Ophiolite melanges (Sadat, 1978).

This region (study area) is located in the northern part of South Khorasan Province (between latitudes 33º 32´ 33.98´´ N to 33° 37´ 57.28´´ N and longitudes 59° 5´ 18.69´´ E to 59º 09´ 54.59´´ E) (Najafi shahali baglu, 2015), in southwestern Qayen and especially west of Anjul village (Fig. 1) (Fig. 2).

According to the 1:100000 geological map of Qayen (Sadat, 1978; Alavi Naini 1981), and (Najafi shahali baglu, 2015) the oldest rock units of this region include gneisses, migmatites, granites, acid metavolcanics, schists, quartzites, and metamorphic limestones attributed to Proterozoic era. Shale and Jurassic sandstones, lower cretaceous limestones, Andesitic lavas, upper cretaceous tuffs, and lenses of ultramafic rocks are other rock units of this area.

The main aim of this research is to specify the primary metamorphic position of an area that has not done in this area to now (Najafi shahali baglu, 2015). Because to present it has not been done any research project about the metamorphism of this area, it is our main idea to specify that in this area. Only one tectonic project has been done in this area and around (Gholami 1999).

Based on the absolute age dating studies (Sadat, 1978; Alavi Naini 1981; Gholami 1999; Zarrinkoub et al. 2010), conducted (from old to recent), the rock units of the study area are including: Jurassic and Pre-Cretaceous rock units that have relatively extensive outcrop in the region (Najafi shahali baglu, 2015). In this region, a rock collection attributed to the Proterozoic era has been introduced that we have named as Zul Complex (Najafi shahali baglu, 2015). Zul is the village where this complex is located.

The rocks forming this complex include: anatexites granites, migmatites, gneisses, and some alabasters (a

[1] Department of Mining Engineering, Faculty of Engineering, University of Birjand, Birjand, Iran, [2] Department of Geology, Faculty of Sciences, University of Birjand, Birjand, Iran
G.R. Fotoohi: gfotohirad@birjand.ac.ir

mineral), amphibolites, and quartzites (Najafi shahali baglu, 2015). Gholami (1999) and Zarrinkoub et al. (2010) have attributed the age of these granites to the Jurassic system. In the western part of Anjul, some disarrays (or transform boundaries) of shale layers among the garnet gneisses (Fig. 3. A). Fig. 3. B shows the boundary of gneisses (Center) and granites (rim) in the field. The main metamorphic rocks of the study area that in this research we have focused on include slates, phyllites, mica schists, garnet mica schists, andalusite schists, andalusite kyanite schists, Sillimanite schists, gneisses (Najafi shahali baglu, 2015; Zarrinkoub et al., 2010) (Fig. 4. A, B, C and D) and some amphibolites (Fig. 5), and metaquartzites (Najafi shahali baglu, 2015).

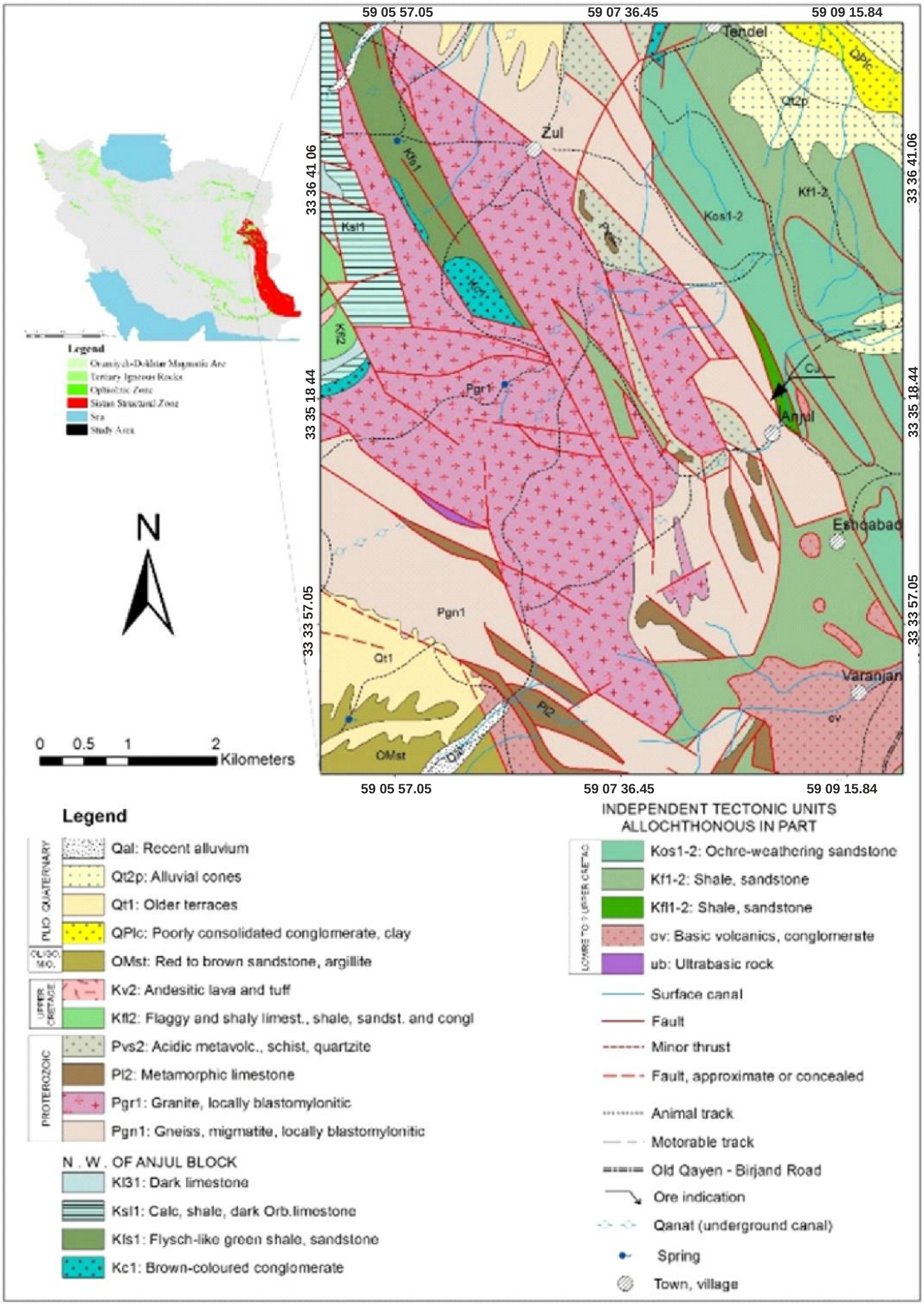

Fig. 2. The geological map of the study area (the main part of study area is in central part of the map that is adapted from (Najafi shahali baglu, 2015)).

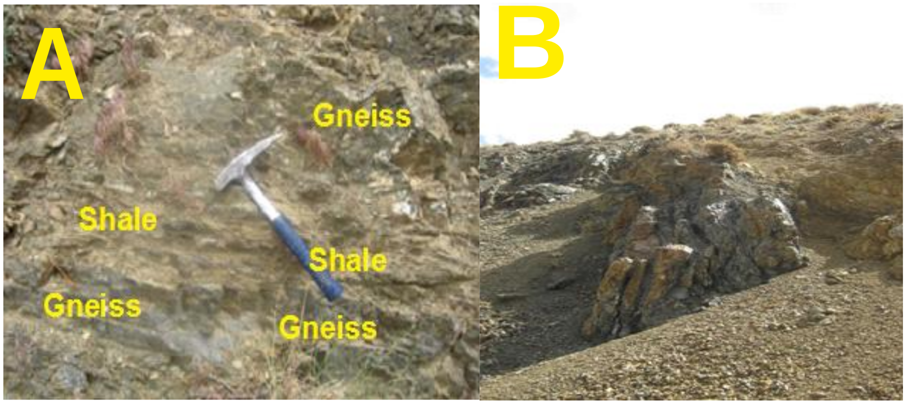

Fig. 3. A: Shale layers among garnet gneisses in the west of Anjul (photo view to northeast), B: The boundary of gneisses (Center) and granites (rim) in field (view to northwest)

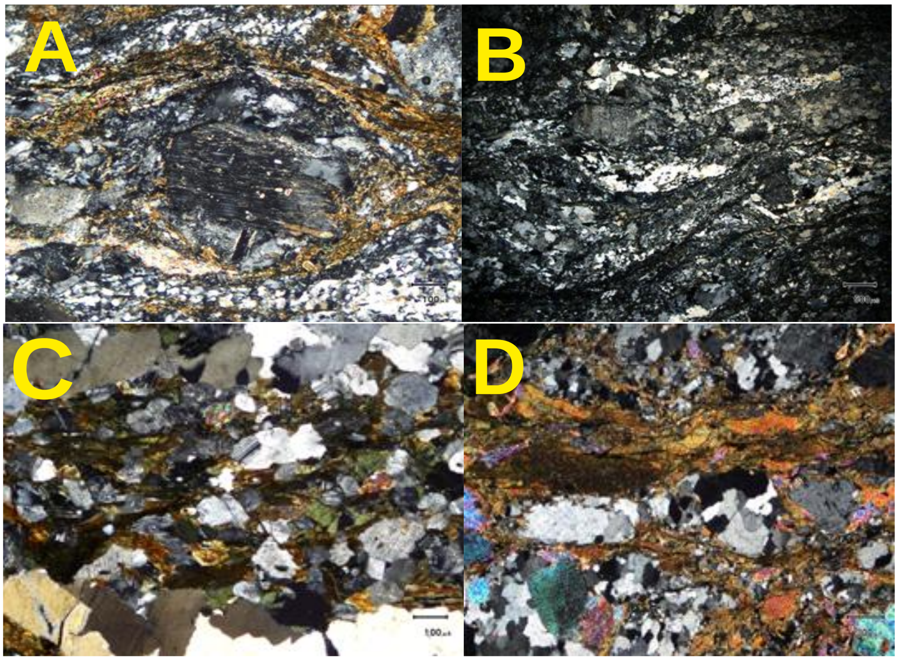

Fig 4. A: Eye feldspar in eye gneisses and rims of biotite and muscovite (XPL), B: Differentiation of quartz in eye gneisses (XPL) C: Locosome (including quartz and feldspars) and melanosome (including biotite and hornblende) in migmatites (XPL) D: Differentiation of biotite from quartz and alkali feldspar in gneiss(XPL) (Najafi shahali baglu, 2015)

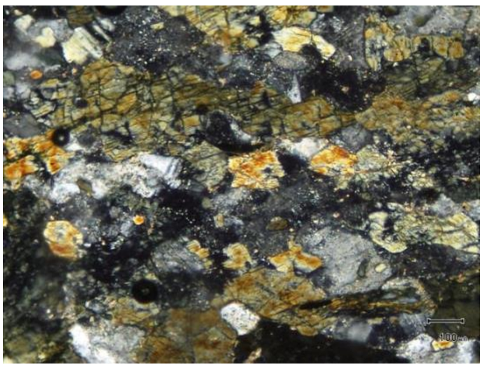

Fig 5. Hornbelende (green) and plagioclase(gray) in amphibolites (XPL) (Najafi shahali baglu, 2015)

II. Methods

The point analysis of some minerals in study the metamorphic rocks of the study area was done at the Iranian Mineral Processing Research Center to determine the type of minerals, their precise naming, zoning study in some minerals types, and applying chemical composition of the minerals of different metamorphic rocks available in this region for determining the temperature and equilibrium crystallization pressure of different minerals of these rocks. These rocks include amphibolites, garnet schists, andalusite kyanite schists and andalusite sillimanite schists. For this idea, an electron probe micro-analyzer (EPMA) was used at the Iranian Mineral Processing Research Center. Since EPMA cannot determine and distinguish Fe2+ and Fe3+ amounts, the Fe of the minerals must be given either as Fe2+ or Fe3+. In the present study, for iron minerals such as Pyroxenes, garnets, and spinels having variable ratios of Fe2+/Fe3+, Fe3+ has been estimated by using the Droop equation

(Droop, 1987) based on the Stoichiometry of the above-mentioned minerals. For all the minerals, the exact determination of structural formula and end members of solid solution minerals was conducted by using the available patterns at the Electron Microprobe Laboratory of the Geology Department at the University of Manchester by Excel software. The results of the microprobe analyses of the minerals of various igneous and metamorphic rocks have been presented in Tables 1-6. For determining the magmatic series, magma chemistry, and magmatic changes of parent original rocks of the amphibolites, garnet schists, andalusite kyanite schists and andalusite sillimanite schists, chemical classification, and determining the original rocks (protoliths), determining their tectonomagmatic environment as well as the changes of their main elements, as many as three samples of the metamorphic rocks of the region were sent to the laboratory of Geological Survey & Mineral Explorations of Iran for chemical analyses by XRF method. The results of these analyses are provided in Table 7. The diagrams have been drawn using Minpet 2.02 and New Pet.

III. MINERAL CHEMISTRY OF METAMORPHIC ROCKS

In this part we present the mineral chemistry of the metamorphic rocks in the study area that have been probed by electron microprobe.

A. A. PYROXENES

The analysis findings of the electron probe micro-analyzer of 4 points of Clinopyroxene in amphibolite sample of the study area are presented in Table 1. Based on the diagram of Fig. 6, Clinopyroxene has an almost uniform composition from the rim toward the center, and it is located in the range of augite. The mineral formula is measured based on four cation and six oxygen.

Table 1. Microprobe analysis results of pyroxenes of Anjul Amphibolite (Najafi shahali baglu, 2015)

Amphibolite				
Oxides	Cpx1	Cpx2	Cpx3	Cpx4
SiO_2	54.54	52.40	48.92	49.26
TiO_2	0.23	0.21	0.99	0.93
Al_2O_3	8.89	2.68	6.47	6.05
Cr_2O_3	0.00	1.04	0.00	0.00
FeO	9.25	3.30	12.02	12.31
MnO	0.03	0.13	0.18	0.17
MgO	6.48	16.49	14.45	14.92
CaO	12.38	22.95	12.15	12.07
Na_2O	7.20	0.35	0.78	0.82
K_2O	0.06	0.00	0.48	0.43
Total	99.06	100.55	96.45	96.97
Mol Props.				
Fomula(corr.)	6(O)	6(O)	6(O)	6(O)
Si	1.985	1.937	1.878	1.879
Ti	0.006	0.006	0.029	0.027
Al	0.381	0.115	0.293	0.272
Cr	0.000	0.030	0.000	0.000
Fe3+	0.147	-0.006	-0.025	-0.003
Fe2+	0.134	0.106	0.411	0.395
Mn	0.001	0.004	0.006	0.005
Mg	0.352	0.892	0.827	0.849
Ca	0.483	0.892	0.500	0.493
Na	0.508	0.025	0.058	0.061
K	0.003	0.000	0.024	0.021
Total	4.000	4.000	4.000	4.000
Mg/(Mg+Fe2+)	0.724	0.894	0.668	0.682
Fe2/Fetot	0.477	1.056	1.065	1.007
Al/(Al+Fe3+Cr)	0.721	0.826	1.093	1.010
End members				
En	0.363	0.472	0.476	0.488
Fs	0.139	0.056	0.236	0.228
Wo	0.498	0.472	0.288	0.284
Jd	0.367	0.020	0.063	0.061
Ac	0.142	0.004	-.0005	-0.001
Aug	0.492	0.975	0.942	0.939

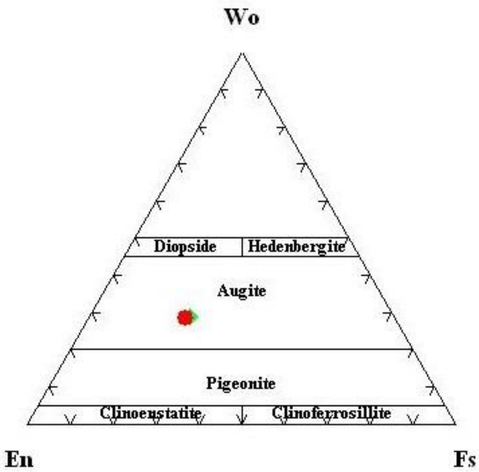

Fig. 6. The composition of the pyroxenes in amphibolite sample in the triangular diagram of pyroxenes (Droop, 1987)

B. Amphiboles

Amphiboles are included as the main minerals in amphibolite rocks. The importance of this mineral is manifested in its variety of composition with different conditions of metamorphism. As can be seen in Figs. 7. A and 7. B, the compositions of this mineral is in the category of calcic amphiboles and can be categorized as magnesiohornblende (Mg# = 0.67 – 0.57). Calcic amphiboles are usually result from progressive metamorphisms and the formation of greenschist facies metamorphic rocks, epidote amphibolite, and at times from amphibolite. Fig. 8 indicates their location in the metamorphic amphiboles zone (Morimoto, 1988).

C. Garnet

Garnet crystals have always been used as an important mineral to study the changes as well as measure the pressure and temperature of metamorphic rocks. Pyralspite garnets (especially those rich in almandine) are found in a variety of rocks from the metamorphic collection of Anjul as well as in neighboring igneous rocks. Although the composition of these minerals is categorized as the chemical composition of almandine mineral (Garnet rich in iron), the amount of pyrope (magnesium) found in them is significant; they were formed during subduction (Fotoohi Rad, 2004; Fotoohi Rad et al., 2005 ; Bröcker et al., 2013). If chlorite and epidote are used, produced garnets will be grossular (Calcium bearing garnets) and almandine –pyrope (iron and magnesium bearing garnets or complex garnets) will be formed. As a result, three component garnets will be produced that have calcium, iron, and magnesium (Figure 9).

Table 2. Microprobe analysis results of amphiboles of Anjul amphibolites (Najafi shahali baglu, 2015)

Oxides	hbl1	hbl2	hbl3	hbl4	hbl5	hbl6	hbl7	hbl8
SiO_2	43.36	46.56	45.98	46.91	48.75	49.56	48.60	49.48
TiO_2	0.34	1.52	1.36	1.23	0.83	0.78	0.58	0.81
Al_2O_3	16.53	9.23	8.06	8.53	6.87	6.61	5.95	6.10
Cr_2O_3	0.01	0.02	0.00	0.03	0.00	0.01	0.01	0.02
FeO	12.48	11.69	11.38	11.85	12.45	12.35	12.73	12.46
MgO	0.01	0.01	0.01	0.01	0.01	0.01	0.01	0.01
CaO	0.01	0.01	0.01	0.01	0.01	0.01	0.01	0.01
Na_2O	0.01	0.01	0.01	0.01	0.01	0.01	0.01	0.01
K_2O	0.01	0.01	0.01	0.01	0.01	0.01	0.01	0.01
Total	100.01	100.01	100.01	100.01	100.01	100.01	100.01	100.01
Mol Props.(M.P.)	.(M.P.)	(M.P.)	(M.P.)	(M.P.)	(M.P.)	(M.P.)	(M.P.)	(M.P.)
Formulas (corr.)	23(O)	23(O)	23(O)	23(O)	23(O)	23(O)	23(O)	23(O)
Si	6.143	6,807	6,936	6,890	6,067	6,167	6,216	6,151
Ti	0,036	0,167	0,154	0,136	0,091	0,085	0065	0,087
Al	2.760	1.590	1.423	1,477	2.76	2.76	2.76	2.76
Cr	0.000	0.000	0.000	0.000	0.000	0.000	0.000	0.000
Fe^{3+}	1.243	0.228	0.071	0.220	0.486	0.335	0.125	0.450
Fe^{2+}	0.236	1.201	1.365	1.226	1.023	1.159	1.456	1.056
Mn	0.005	0.021	0.023	0.022	0.023	0.023	0.025	0.026
Mg	2.577	2.986	2.76	3.018	3.019	3.136	3.104	3.072
Ca	1,632	1.891	3.018	1.917	1.876	1.893	2.014	1.880
Na	0.338	0.320	1.954	0.290	0.194	0.179	0.178	0.202
K	0.036	0.132	0.129	0.127	0.078	0.068	0.066	0.072
Total	15,006	15,343	15,361	15,335	15,148	15,141	15,259	15,153
$Mg/(Mg+Fe^{2+})$	0.916	0.713	0.689	0.710	0.754	0.728	0.678	0.751
Fe^{2+}/Fe_{tot}	0.159	0.840	0.950	0.849	0.687	0.776	0.921	0.701
$Al/(Al+Fe^{3+}+Cr)$	0.690	0.874	0.953	0.870	0.707	0.771	0.893	0.698

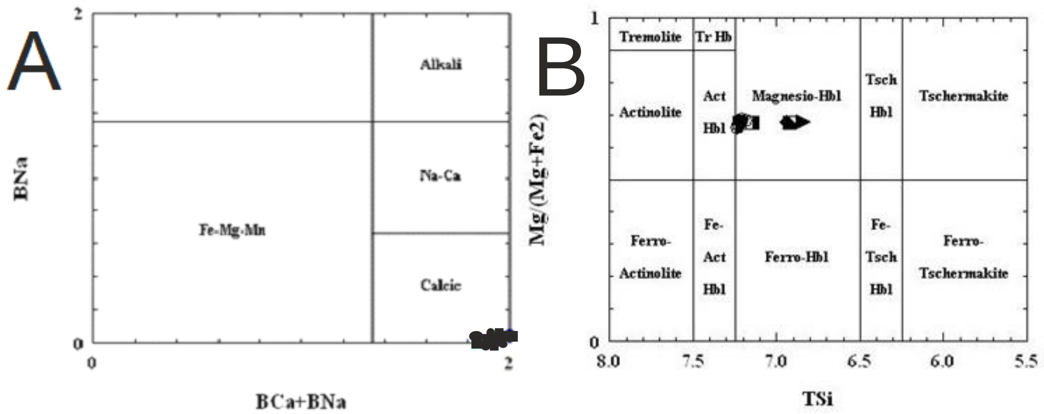

Fig. 7. (A) The Calcic composition of amphiboles of Anjul amphibolites, and (B) The almost similar composition of amphiboles of Anjul metamorphic rocks (Leake, 1997)

Table 3. Microprobe analysis results of garnets of Anjul metamorphic rocks (Najafi shahali baglu, 2015)

	grt1	grt2	grt3	grt4	grt5	grt6	grt7	grt8	grt9	grt10
Oxides	Garnet Schist				Andalusite Sillimanite Schist			Andalusite(this mineral is relict) Kyanite Schist		
SiO_2	37.85	36.68	36.51	35.95	56.33	35.85	37	36.81	35.87	36.82
TiO_2	0.01	0.03	0.13	0.04	0.01	0.03	0.02	0.00	0.00	0.02
Al_2O_3	21.6	20.93	21.39	20.83	21.27	20.77	19.74	20.56	20.95	21.12
Cr_2O_3	0.00	0.00	0.00	0.00	0.00	0.00	0.00	0.00	0.00	0.00
FeO	32.52	29.99	29.52	29.8	31.07	30.85	29.72	30.63	31.77	30.8
MnO	1.10	1.78	1.62	1.62	3.5	5.07	4.92	4.94	3.64	4.12
MgO	6.02	4.86	5.22	5.02	3.72	2.99	2.84	3.16	3.72	3.57
CaO	0.79	4.51	4.8	5.46	3.41	3.38	4.79	2.78	3.17	2.81
Total	99.90	99.04	99.59	99.21	99.55	99.25	99.21	98.97	99.48	99.19
Fomula(corr.)	12(O)	12(O)	12(O)	12(O)	12(O)	12(O)	12(O)	12(O)	12(O)	12(O)
Si	2.990	2.933	2.895	2.871	2.919	2.911	3.000	2.989	2.894	2.956
Ti	0.001	0.002	0.008	0.002	0.001	0.002	0.001	0.000	0.000	0.001
Al	2.011	1.973	1.999	1.961	2.14	1.988	1.886	1.967	1.992	2.009
Cr	0.000	0.000	0.000	0.000	0.000	0.000	0.000	0.000	0.000	0.000
Fe^{3+}	0.007	0.157	0.194	0.291	0.145	0.187	0.111	0.055	0.220	0.76
Fe^{2+}	2.141	1.849	1.763	1.699	1.943	1.908	1.904	2.025	1.924	2.003
Mn	0.074	0.121	0.109	0.110	0.238	0.349	0.338	0.340	0.249	0.282
Mg	0.709	0.579	0.617	0.598	0.446	0.362	0.343	0.382	0.447	0.430
Ca	0.067	0.386	0.414	0.467	0.294	0.294	0.416	0.242	0.274	0.243
Total	8.000	8.000	8.000	8.000	8.000	8.000	8.000	8.000	8.000	8.000
$Mg/(Mg+Fe^{2+})$	0.249	0.239	0.259	0.260	0.187	0.159	0.153	0.159	0.189	0.177
$Fe^2/(Fe^2+Fe^3)$	0.997	0.922	0.901	0.854	0.930	0.911	0.945	0.973	0.897	0.963
$Al/(Al+Fe^3+Cr)$	0.996	0.926	0.911	0.871	0.933	0.914	0.944	0.973	0.901	0.963
End members										
Almandine	71.6	63.0	60.7	59.1	66.5	65.5	63.4	67.7	66.5	67.7
Spessartine	2.5	4.1	3.7	3.8	8.2	12.0	11.3	11.4	8.6	9.5
Pyrope	23.7	19.7	21.3	20.8	15.3	12.4	11.4	12.8	15.5	14.5
Grossular	2.2	12.2	13.0	14.2	9.4	9.2	13.1	7.9	8.5	7.9
Andradite	0.0	1.0	1.3	2.1	0.7	0.9	0.8	0.2	9.0	0.3
Uvarovite	0.0	0.0	0.0	0.0	0.0	0.0	0.0	0.0	0.0	0.0

The changes in the composition of garnets are studied in different crystals and within the crystals themselves. The definite zoning of garnets based on Table 3 (increasing in amount of magnesium and decreasing in the amount of manganese and iron from the core toward the rim), can indicate the growth of these garnets has been as well as the crystallization depth increase from the core toward the rim (Bröcker et al. 2013; Kurzawa et al. 2017). This zoning can indicate the growth of garnets during the subduction process (Kurzawa et al., 2017 ; Hyndman, 1985). This distribution is affected by metamorphism degree, temperature, cooling rate, the fluid nature, and the chemistry of the protolith. In garnets of garnet schist, andalusite kyanite schist, and andalusite-sillimanite schist, the amount of almandine, pyrope, spessartine, and grossular are 63.4, 15.3, 8.2, and 7.9 percent respectively. This kind of chemical zoning is specific to metamorphic garnets with high intensity (Hyndman, 1985). Fig. 10 indicates the location of garnets of metamorphic rocks of the study area in the Klein diagram (Bröcker et al., 2013; Zheng et al., 2007; Aoya, 2001).

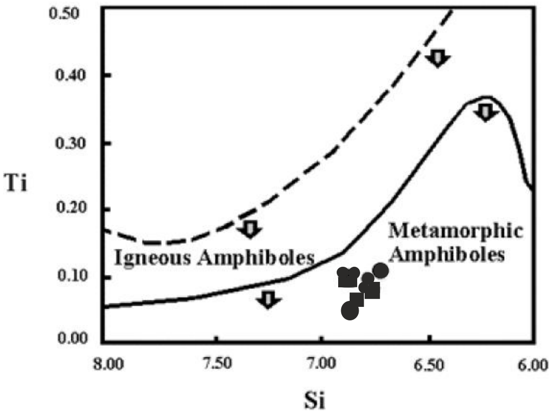

Fig. 8. The location of amphiboles in the rocks studied within the category of metamorphic amphiboles (Leake, 1978)

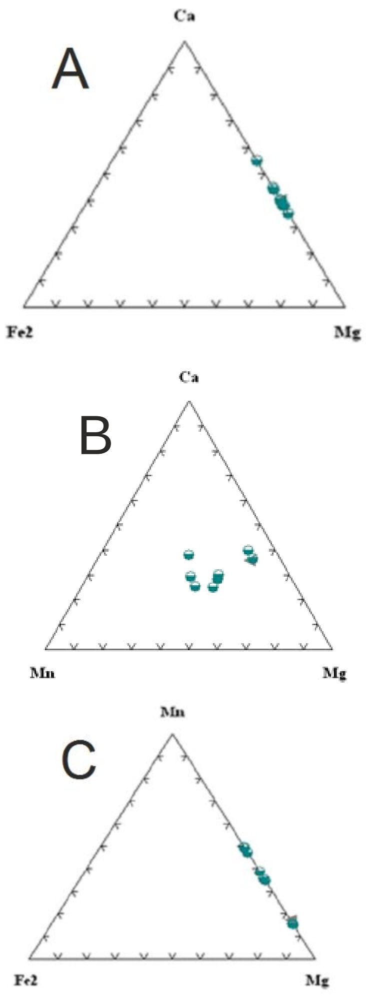

Fig 9. The chemical composition of garnet in A. andalusite kyanite schists, B. Andalusite-Sillimanite schists, and C. mica schists in Anjul area

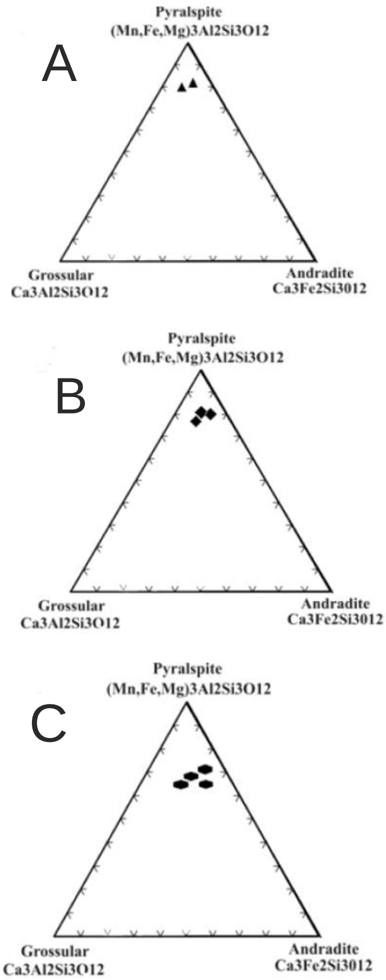

Fig. 10. The compositional location of garnets of the metamorphic rocks: A. Andalusite-kyanite schist; B. mica garnet schist; and C. Andalusite-Sillimanite schist in Pyralspite zone (Bröcker et al., 2013)

D. Feldspars

Feldspars found in samples of andalusite-sillimanite schists, garnet schists, and andalusite-kyanite schists of the study area are of two types: sodium and calcium-bearing feldspars. Moreover, feldspars in the andalusite-sillimanite schist metamorphic rocks are of potassium feldspar type. Alkali feldspar of the region is orthoclase. The labradorite composition of plagioclases shows amphibolite facies of metapelitic rocks of the area and orthoclase must be relict of parent rocks before metamorphism in this area. Table 4 shows the results of microprobe analysis of Plagioclase minerals of metamorphic rocks of Anjul. Table 5 indicates the results of microprobe analysis of Orthoclase minerals of metamorphic rocks of Anjul. The composition of Plagioclases available in amphibolites in the triangular classification of Albite-Orthoclase-Anorthite is categorized in the category of Andesine-Labradorite intermediate Plagioclases (XAn=70.07 – 63.30). Figure 11 indicates the distribution pattern of feldspars.

Table 4. Microprobe analysis results of feldspars of Anjul metamorphic rocks (Najafi shahali baglu, 2015)

	Andalusite Kyanite Schist			Andalusite Sillimanite Schist			Garnet Schist		
SiO_2	68.11	54.7	54.34	54.7	53.75	65.84	65.76	54.49	55.83
TiO_2	0.00	0.00	0.03	0.03	0.03	0.00	0.03	0.00	0.02
Al_2O_3	19.29	27.66	28.14	26.69	26.30	18.85	18.95	27.60	26.91
Cr_2O_3	0.00	0.00	0.00	0.00	0.00	0.00	0.00	0.00	0.00
FeO	0.05	0.02	0.12	0.32	0.43	0.10	0.09	0.00	0.03
MnO	0.06	0.02	0.03	0.00	0.02	0.01	0.01	0.01	0.01
MgO	0.00	0.01	0.00	0.00	0.24	0.00	0.02	0.00	0.00
CaO	0.21	10.61	10.98	11.97	11.74	0.00	0.01	11.10	9.95
Na_2O	11.95	4.98	5.62	5.56	5.02	0.09	0.12	5.91	5.72
K_2O	0.02	0.18	0.11	0.66	1.68	13.9	14.06	0.16	0.08
Total	99.73	98.26	99.35	99.93	99.23	98.79	99.07	99.28	98.56
Formula	8(O)	8(O)	8(O)	8(O)	8(O)	8(O)	8(O)	8(O)	8(O)
Si	2.989	2.505	2.472	2.493	2.481	3.026	3.018	2.484	2.544
Ti	0.000	0.000	0.000	0.001	0.0001	0.000	0.001	0.000	0.001
Al	0.998	1.493	1.509	1.434	1.431	1.021	1.025	1.483	1.445
Cr	0.001	0.000	0.000	0.000	0.000	0.000	0.000	0.000	0.000
Fe^{2+}	0.002	0.001	0.005	0.012	0.017	0.004	0.003	0.000	0.001
Mn	0.002	0.001	0.001	0.000	0.001	0.000	0.000	0.000	0.000
Mg	0.000	0.001	0.000	0.000	0.017	0.000	0.002	0.000	0.000
Ca	0.010	0.521	0.535	0.585	0.581	0.000	0.000	0.542	0.486
Na	1.017	0.442	0.496	0.491	0.450	0.008	0.012	0.522	0.506
K	0.001	0.011	0.006	0.038	0.099	0.815	0.823	0.009	0.005
Total	5.020	4.974	5.024	5.054	5.077	4.875	4.886	5.041	4.988
Na/(Na+K+Ca)	0.989	0.454	0.478	0.441	0.398	0.010	0.014	0.486	0.508
K/(Na+K+Ca)	0.001	0.011	0.006	0.034	0.088	0.990	0.986	0.009	0.005
Ca/(Na+K+Ca)	0.010	0.535	0.516	0.525	0.514	0.000	0.001	0.505	0.487

Table 5. Microprobe analysis results of orthoclases of Anjul metamorphic rocks (Najafi shahali baglu, 2015)

	Ab1	rim	center
	Andalusite- Sillimanite Schist		
SiO_2	68.11	65.84	65.76
TiO_2	0.00	0.00	0.003
Al_2O_3	19.29	18.85	18.95
Cr_2O_3	0.04	0.00	0.00
FeO	0.05	0.01	0.09
MnO	0.06	0.01	0.01
MgO	0.00	0.00	0.03
CaO	0.21	0.00	0.01
Na_2O	11.95	0.09	0.13
K_2O	0.02	13.90	14.06
Total	99.73	98.79	99.0
Oxygene prop.			
SiO_2	2.2671	2.1916	2.1889
TiO_2	0.0000	0.0000	0.0008
Al_2O_3	0.5676	0.5546	0.5576
Cr_2O_3	0.0008	0.0000	0.0000
FeO	0.0007	0.0014	0.0013
MnO	0.0008	0.0001	0.0001
MgO	0.0000	0.0000	0.0007
CaO	0.0037	0.0000	0.0002
Na_2O	0.1928	0.0015	0.0021
K_2O	0.0002	0.1476	0.1493
Total	3.0338	2.8968	2.9009
Norm. factor	2.637	2.762	2.758
Na/(Na+K+Ca)	0.989	0.010	0.014
K/(Na+K+Ca)	0.001	0.990	0.986
Ca/(Na+K+Ca)	0.010	0.000	0.001

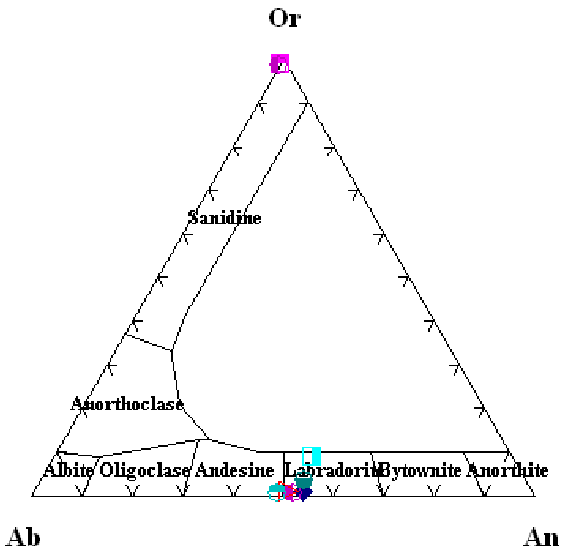

Fig. 11. The composition of Feldspars in the metamorphic sample of Andalusite-Sillimanite schist in the triangular diagram of Or-Ab-An (Zheng et al., 2007)

E. BIOTITES

Biotites are found with some brown colors and as very small to medium-size crystals along the fractures of feldspars and in the matrix of andalusite-sillimanite schists, andalusite-kyanite schists, and garnet schists. Based on the classification of Foster (Aoya, 2001), these biotites are categorized as iron-rich biotites (Fig. 12). The composition of bioties is placed in the field of the end member of biotite (Table 6 and Fig. 13).

Determination of Magmatic series and the tectonic setting of amphibolite protolith by using Pyroxene chemical composition

Given the views of Le Bas (2000), the amounts of Si, Al, and Ti with the structural network of Pyroxene depend on the alkaline degree, and by using this feature, magma series are distinguished from each other. By using amounts of SiO2 and Al2O3 in the chemical compositions of amphibolite Pyroxenes, Le Bas (2000) has managed to distinguish peralkaline, alkaline, and subalkaline magma series of the original rock of these metamorphic rocks. According to Fig. 14, owing to the lack of TiO2 the original rock of most of the samples is categorized as igneous calc-alkaline rocks. The results of the microprobe analysis of amphibolite pyroxenes have been presented in Table 7.

Table 6. Microprobe analysis results of biotites of Anjul metamorphic rocks (Najafi shahali baglu, 2015)

	bio1	bio2	bio3	bio4	bio5	bio6	bio7	bio8	bio9	bio10	bio11
		Andalusite Kyanite Schist				Andalusite Sillimanite Schist			Garnet Schist		
SiO_2	54.74	34.32	35.54	35.07	34.55	33.91	33.57	33.82	34.86	33.80	34.67
TiO_2	0.17	2.69	2.69	2.06	2.16	2.25	2.49	2.92	2.23	2.44	2.79
Al_2O_3	19.65	19.51	20.06	20.02	19.52	18.78	19.82	19.54	18.92	18.75	18.59
Cr_2O_3	0.00	0.00	0.00	0.00	0.00	0.00	0.00	0.00	0.00	0.00	0.00
FeO	3.60	18.07	18.25	17.47	18.18	18.17	18.87	17.99	18.13	18.51	18.55
MnO	0.00	0.21	0.20	0.20	0.23	0.28	0.22	0.22	0.10	0.10	0.10
MgO	5.76	9.15	9.55	9.83	9.14	9.86	9.51	9.63	10.32	9.87	10.00
CaO	0.00	0.00	0.00	0.00	0.00	0.00	0.00	0.00	0.00	0.00	0.00
Na_2O	0.03	0.32	0.41	0.13	0.25	0.16	0.19	0.12	0.24	0.43	0.24
K_2O	11.28	9.61	9.27	9.75	10.05	10.79	9.72	9.78	9.39	9.84	9.71
Total	95.23	93.88	95.99	94.59	94.17	94.24	94.43	94.08	94.20	93.78	94.69
Formula	11(O)	11(O)	11(O)	11(O)	11(O)	11(O)	11(O)	11(O)	11(O)	11(O)	11(O)
Si	3.687	2.515	2.535	2.543	2.530	2.499	2.456	2.479	2.540	2.492	2.523
Ti	0.09	0.148	0.144	0.112	0.119	0.125	0.137	0.161	0.122	0.135	0.153
Al	0.1560	1.685	1.686	1.711	1.685	1.631	1.709	1.688	1.625	1.630	1.595
Cr	0.000	0.000	0.000	0.000	0.000	0.000	0.000	0.000	0.000	0.000	0.000
Fe^{3+}	0.000	1.107	1.089	1.059	1.113	1.120	1.155	1.103	1.105	1.141	1.129
Fe^{2+}	0.203	0.000	0.000	0.000	0.000	0.000	0.000	0.000	0.000	0.000	0.000
Mn	0.000	0.013	0.012	0.014	0.017	0.014	0.014	0.014	0.006	0.006	0.006
Mg	0.578	1.000	1.015	1.062	0.998	1.083	1.037	1.052	1.121	1.085	1.085
Ca	0.000	0.000	0.002	0.001	0.005	0.023	0.027	0.017	0.034	0.061	0.034
Na	0.000	0.000	0.000	0.000	0.000	0.000	0.000	0.000	0.000	0.000	0.000
K	0.969	0.898	0.844	0.902	0.939	1.014	0.907	0.914	0.873	0.926	0.902
Total	7.011	7.421	7.383	7.420	7.439	7.520	7.442	7.431	7.426	7.480	7.430
$Mg/(Mg+Fe^{2+})$	0.740	1.000	1.000	1.000	1.000	1.000	1.000	1.000	1.000	1.000	1.000
$Al/(Al+Fe^{3+}+Cr)$	1.000	0.603	0.608	0.618	0.602	0.593	0.597	0.605	0.595	0.588	0.585
Na/(Na+K)	0.004	0.048	0.063	0.020	0.036	0.022	0.029	0.018	0.037	0.062	0.036

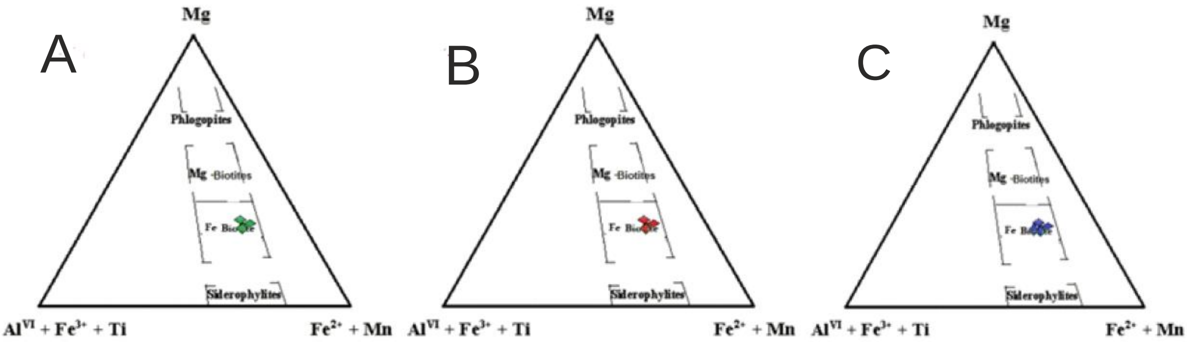

Fig. 12. A. metamorphic biotites, garnet schists, B. Andalusite-kyanite schists, C. Andalusite-Sillimanite schists of Anjul area that is located in the iron rich biotite field (Tracy, 1982)

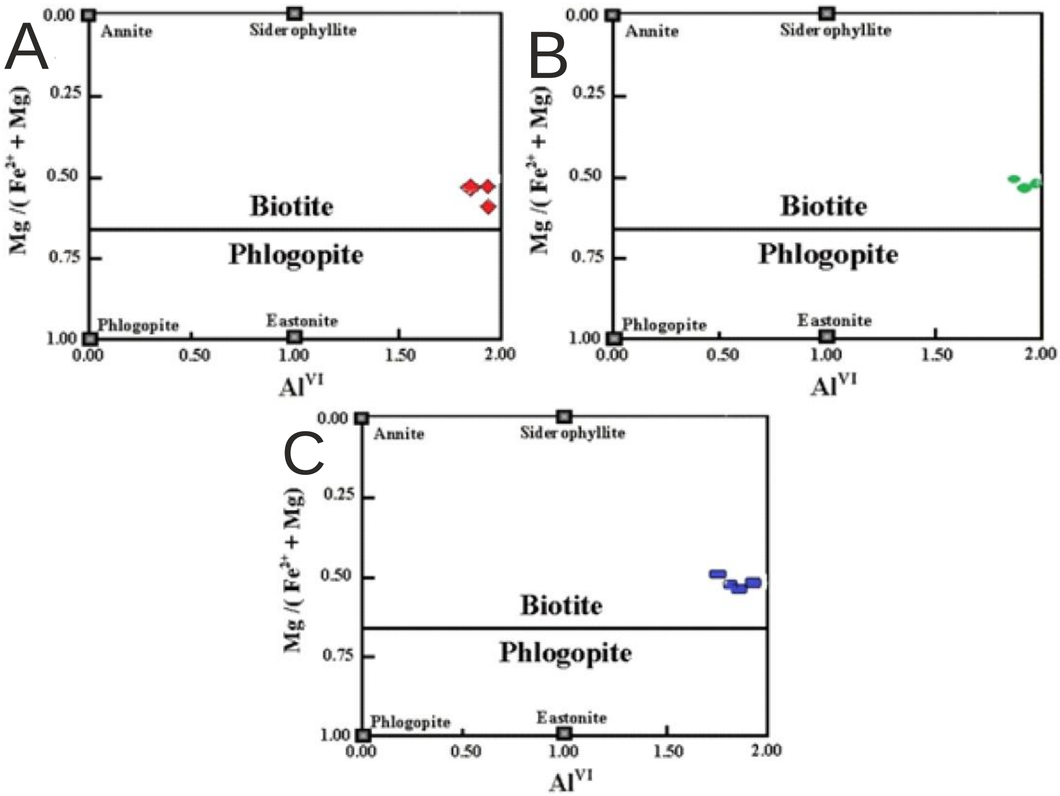

Fig. 13. (A) Determination of metamorphic biotite composition, garnet schists, (B) Andalusite-kyanite schists, and (C) Andalusite-Sillimanite schists of Anjul in Deer Diagram (Deer, 1992)

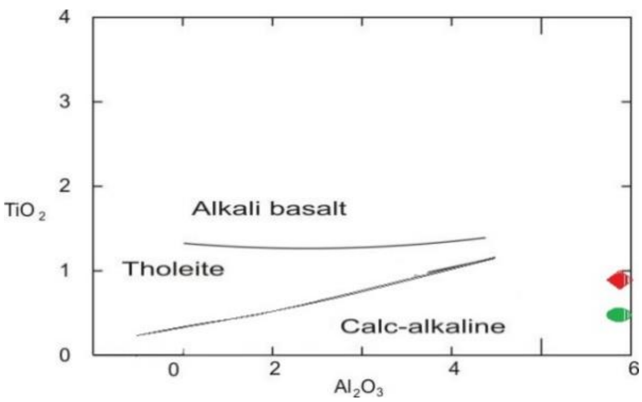

Fig. 14. The diagram of Al2O3 versus TiO2 of relict pyroxenes of parent rock in amphibolite (Le Base, 2000)

IV. Protolith of the Studied Metamorphic Rocks

On the basis of the field studies as well as the study of thin sections, we came to the conclusion that the protolith of the metamorphic rocks of the region mainly were greywacke, acid tuffs, arkoses, pelitic rocks and basalts (gabbros). For confirming findings obtained from macroscopic and microscopic studies, the following diagrams were also used for determining the origin of these rocks.

A. Triangular diagram MgO-K2O-Na2O (La Roche, 1965)

As seen in this diagram, the protolith of amphibolites is categorized as gabbro and the protolith of gneisses is categorized as granodiorite (greywacke) and rhyolite (Fig. 15).

B. SiO2 Diagram (MgO+FeO+Fe2O3) (Petijan, 1949)

In this diagram, the protolith of the metamorphic rocks are categorized as greywacke, granite, arkose, pelite, and basalt. In this diagram, the samples that are categorized as granite are anatexites, and those samples that are categorized as basalt are amphibolites (Fig. 16).

On the basis of the field and laboratory studies, two different kinds of metamorphisms can be observed in this area: regional and dynamic metamorphism. Among the different metamorphic rocks observed in this area, we can refer to slate, schist, amphibolite, mylonite, gneiss, and migmatite.

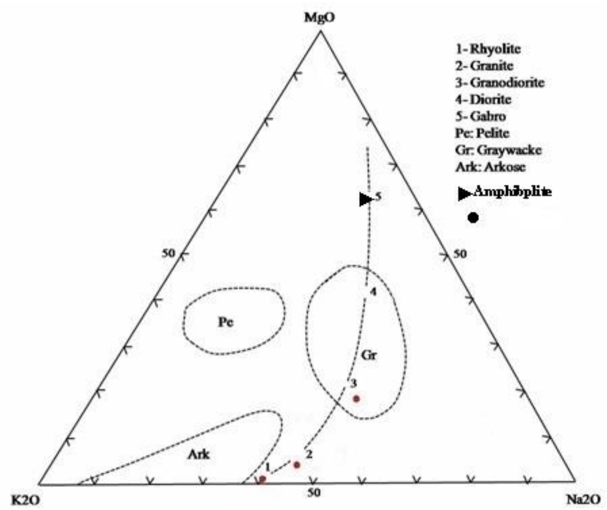

Fig. 15. Triangular diagram of Laroche (La Roche, 1965) for determining the protolith of the metamorphic rocks of the study area. The circles in the Fig. are the protolith composition of gneisses samples.

V. Conclusions

According to the present study, the findings are as follows:

- Clinopyroxenes belonging to amphibolites of Anjul almost have a uniform composition from the rim toward the center and are located in the range of an augite. This mineral is igneous relict of the parent rock.

-Amphiboles are calcic amphiboles (magnesiohornblende) and are categorized as metamorphic amphiboles.

- Garnets in garnet schists, andalusite-kyanite schists, and andalusite-sillimanite schists belong to the category of pyralspite type.

- Chemical zoning of garnets confirms the existence of metamorphic garnets with a high metamorphism degree in the study area.

- Feldspars in the samples of Andalusite-kyanite schists, garnet schists, and Andalusite-Sillimanite schists of the area are of two kinds: sodium and calcium-rich feldspars .

- The composition of plagioclases found in amphibolites in the triangular classification of Albite-Orthoclase-Anorthite is categorized in the category of Andesine-Labradorite as intermediate Plagioclases that shows medium grade of metamorphism in these rocks.

-Biotites of the metamorphic rocks, andalusite-kyanite schists, garnet schists, and andalusite-sillimanite schists belong to the category of iron biotites. Elements of iron and titanium constitute an important part of the structure of biotites in this region. The composition of biotites is located in the extension of the end member of the biotite.

- The chemical composition of the pyroxenes in amphibolites supports the igneous protolith with calc-alkaline magma series for these rocks.

- The chemical composition of the rock samples studied indicates that the protolith of amphibolites has been gabbro, and the protolith of gneisses has been granodiorite (greywacke) and rhyolite.

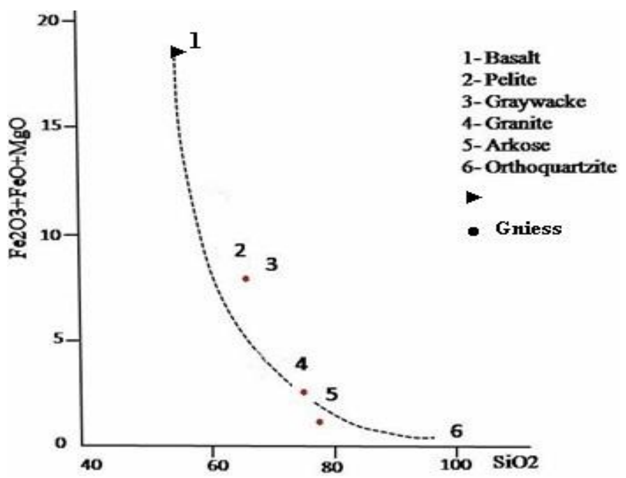

Fig. 16. Pettijohn diagram (Pettijohn, 1949) for determining the protolith of the metamorphic rocks of the study area. Triangle (1) is number 1-Basalt.

REFERENCES

Tirrul, R., Bell, I.R., Griffis, R.J., Camp, V.E. (1983). The Sistan suture zone of eastern Iran. Geological Society of America Bulletin, 49, 134-150.

Nowgol sadat, M.M.A. (1978). Les zones de decrochements et les virgation structurales en Iran, Consequences des resultants de analyse Structurale de la region de Qom, These unive, Scientifique et Medicale de Grenoble, 201 p.

Najafi shahali baglu, H. (2015). Petrology of Anjul metamorphic rocks (southwest of Qayen)- East of Iran. Thesis for master science in petrology, Department of Geology, Faculty of Sciences, The university of Birjand , Birjand, Iran. In Persian. 175 p.

Alavi Naini, M. (1981), Qayen geological map, scale: 1:100000, series, sheet 7857, Supervised by: M. Alavi Naeini, Geological survey of Iran, Tehran, Iran.

Gholami, E. , 1999, The geodynamic research of south western area of Qayen. Thesis for master science in tectonic, Department of Geology, Faculty of Sciences, The university of Tarbiat modarres , Tehran, Iran. In Persian. 175 p.

Zarrinkoub , M.H., Sun-Lin Chung, H.Y., Chiu, S.S., Mohammadi, M.M., Khatib I.J., Lin. (2010.). Zircon U-Pb age and geochemical constraints from the northern Sistan suture zone on the Neotethyan magmatic and tectonic evolution in eastern Iran.

Droop, G.T.R. (1987). A general equation for estimating Fe^{3+} concentrations in ferromagnesian silicates and oxides from microprobe analyses, using stoichiometric criteria. Mineral. Mag. 51, 431-435.

Morimoto N. (1988). Nomenclature of pyroxenes, Mineralogical Magazine, 52, 535-552.

Leake, B.E., et al. (1997). Nomenclature of amphiboles: report of the Subcommittee on Amphiboles of the International Mineralogical Association on New Minerals and Mineral Names. Min. Mag. 61, 295–321.

Leake, B.E. (1978). Nomenclature of amphiboles, American Mineralogist,63, 1023-1052.

Fotoohi Rad, G.R. (2004). Petrology and geochemistry of metamorphosed ophiolites of Eastern Birjand, Ph.D Thesis, Tarbiat Moallem University- in Persian (known as Kharzmi University at present).

Fotoohi Rad, G.R., Droop, G.T.R., Amini, S., Moazzen, M. (2005). Eclogites and blueschists of the Sistan Suture Zone, eastern Iran: a comparison of P-T histories from a subduction

Bröcker, M., Fotoohi, Ra.d.G., Abbaslu, F., Rodionov, N. (2013). Geochronology of highgrade metamorphic rocks from the Anjul area, Lut block, eastern Iran. J Asian Earth Sciences. 82, 151–162.

Kurzawa, T., Broecker, M., Fotoohi Rad, GR., Berndt, J., Lisker, F. (2017). Cretaceous high-pressure metamorphism and low pressure overprint in the Sistan Suture Zone, eastern Iran: Additional temperature estimates for eclogites, geological significance of U-Pb zircon ages and Rb-Sr constraints on the timing of exhumation.

Hyndman, D.W. (1985). Petrology of igneous and metamorphic rocks. Second edition. Mc Graw- Hill Book Company, 786p.

Zheng, L.S., Saleeby, J.B. Ducea, M. (2007). Geochemical characteristic of crustal anatexis during the formation of migmatite at the southern Sierra Nevada, California. Contributions to Mineralogy and Petrology, 150, 386-452.

Aoya, M. (2001). P-T-D path of eclogite from the Sanbagawa belt deduced from petrological and microstructural analyses. Journal of Petrology, v. 42, p. 1225-1248.

Tracy, R.J. (1982). Compositional zoning and inclusions in metamorphic minerals. Rev. Mineral. ,10, 355-397.

Deer, W.A., Howie, R.A. and Zussman, J. (1992). An introduction to the rock-forming minerals. Harlow; Longman. 2 nd edn. John Wiley and Sons, New York, 696p.

mélange. Lithos 84, 1–24.

Le Base, M.J. (2000). IUGS classification of the high Mg and picritic volcanic rocks. Journal of Petrology, 41, 2467- 2470.

La Roche, H. (1965). Existance de pluseurs facies geochemiques dans pes schistes Paleozoic des Pyrenees Lauchonnaises. Ge.Rdschau 55, p. 274-301.

Pettijohn, F.L. (1949). Sedimentary rocks. Harper and brothers, Newyork.